

Ag Decorated Hierarchical Structured ZnO Microspheres and Their Enhanced Electrochemical Performance for Lithium Ion Batteries

X. H. Huang^{*}, J. B. Wu^{*}, Y. Lin, R. Q. Guo, W. W. Zhong

College of Physics & Electronic Engineering, Taizhou University, Taizhou, 318000, China

^{*}E-mail: drhuangxh@hotmail.com; wujb@tzc.edu.cn

Received: 21 August 2014 / Accepted: 18 September 2014 / Published: 29 September 2014

Hierarchical structured ZnO microspheres are prepared by a simple hydrothermal method. These microspheres are then decorated with Ag nanoparticles by electroless silver plating technique. The materials are characterized by means of X-ray diffraction, scanning electron microscopy and energy dispersive spectroscopy. The electrochemical performances as anode materials for lithium ion batteries are investigated by galvanostatic discharge-charge cycle and cyclic voltammetry tests. Ag decorated hierarchical structured ZnO microspheres exhibit an initial charge capacity of 630 mAh g⁻¹ and a stable capacity retention property. They also exhibit better rate capability than pure ZnO microspheres without Ag plating. It is believed that the hierarchical structure of ZnO and the decoration of Ag nanoparticles play important roles in the enhanced electrochemical performance.

Keywords: ZnO, Ag nanoparticle, Hierarchical structure, Microsphere, Lithium ion battery.

1. INTRODUCTION

Transition-metal oxides, such as FeO, CoO, NiO, Cu₂O and ZnO, have attracted much attention as anode materials for lithium ion batteries due to their much higher theoretical capacities than graphite-based materials [1–12]. Among these oxides, ZnO is relatively inexpensive, but it is rarely studied as electrode materials of lithium ion batteries, because it often shows low actual capacity and very poor cycling performance, for example, dropping to below 200 mAh g⁻¹ in just a few cycles. The poor electrochemical performances are attributed to the low conductivity and the pulverization caused by the volume changes during the cycle. To improve the performance, preparing nanostructured materials and forming composite with carbon or metal are often used [13–18], but up to now, few significant achievements have been obtained.

Hierarchical structured materials can exhibit enhanced electrochemical properties when used as lithium ion electrode materials. These materials often have micro-sized primary particles, which are constructed by many ordered secondary or tertiary nanoparticles. Hierarchical electrode materials have both of the advantages of micro-sized and nano-sized particles, such as high tap density, good particle contact and large specific surface area. Furthermore, the hierarchical electrode materials can offer large electrode/electrolyte interfaces, short diffusion paths of lithium ions, and loose structures to avoid agglomeration and pulverization, so these materials exhibit enhanced performances [19–22].

Based on these considerations, in the present work, hierarchical structured ZnO microspheres have been prepared by a simple hydrothermal method, and then they are decorated with Ag nanoparticles by an electroless silver plating technique. The electrochemical performances of this Ag decorated hierarchical structured ZnO microspheres used as anode materials of lithium ion batteries are investigated in detail.

2. EXPERIMENTAL

Hierarchical structured ZnO microspheres were prepared by a hydrothermal method. In a typical synthetic process, 1.12 g zinc nitrate hexahydrate, 0.45 g urea and 0.11 g trisodium citrate dihydrate were dissolved in 75 mL distilled water to form a homogeneous clear solution. The solution was transferred into a 100 mL Teflon-lined stainless steel autoclave and heated at 120 °C for 6 h. The precipitate was collected and washed with distilled water for several times. After dried, the precursor was put into a tube furnace and calcined at 350 °C in air for 45 min.

ZnO microspheres were decorated by Ag nanoparticles using an electroless silver plating technique. The plating solution contains 50 mL freshly prepared 0.01 M $\text{Ag}(\text{NH}_3)_2\text{NO}_3$ solution, 1.0 g polyvinylpyrrolidone (PVP, K30), and 50 mL ethanol. The solution was sealed with a polyethylene film and placed in a water bath at 70 °C for 3 h. Finally, the product was centrifuged, washed with distilled water for three times, and dried in vacuum at room temperature.

The structure of materials were characterized by X-ray diffraction (XRD, Bruker D8 advance; Cu $K\alpha$ radiation). The morphology was observed by scanning electron microscopy (SEM, Hitachi S4800). The elementary composition was analyzed by energy dispersive spectrometer (EDS) equipped in the scanning electron microscope.

Working electrode was prepared by a slurry-coating procedure. Active materials, carbon black and polyvinylidene fluoride (PVDF) were mixed at the mass ratio of 80:12:8. N-methylpyrrolidone (NMP) was added to the mixture under continuous stirring at 60 °C for 1 h to form a homogenous black slurry. The slurry was spread on a copper foam current collector. Finally, the electrode was dried at 100 °C in vacuum for 12 h and pressed under 20 MPa.

Test cells were assembled in an argon-filled glove box (Mikrouna Super) in which the concentrations of water and oxygen were controlled below 1 ppm. The working electrode, the monolayer polypropylene (PP) separator, and the pure lithium foil were stacked in turn inside the CR2025 coin-type cell, and 50 μL of electrolyte (1 M LiPF_6 in EC/DMC) was injected into the cell. The cell was sealed and aged for 12 h before the electrochemical tests.

The cells were discharge-charged repeatedly on a program-control battery testing system (MTI BST8-3) using different current densities of 50, 100, 200 and 500 mA g⁻¹ between two cut-off voltages of 0.1 and 3 V. Cyclic voltammetry (CV) tests were conducted on an electrochemical workstation (CHI600D) at a scan rate of 0.1 mV s⁻¹ between 0 and 3 V.

3. RESULTS AND DISCUSSION

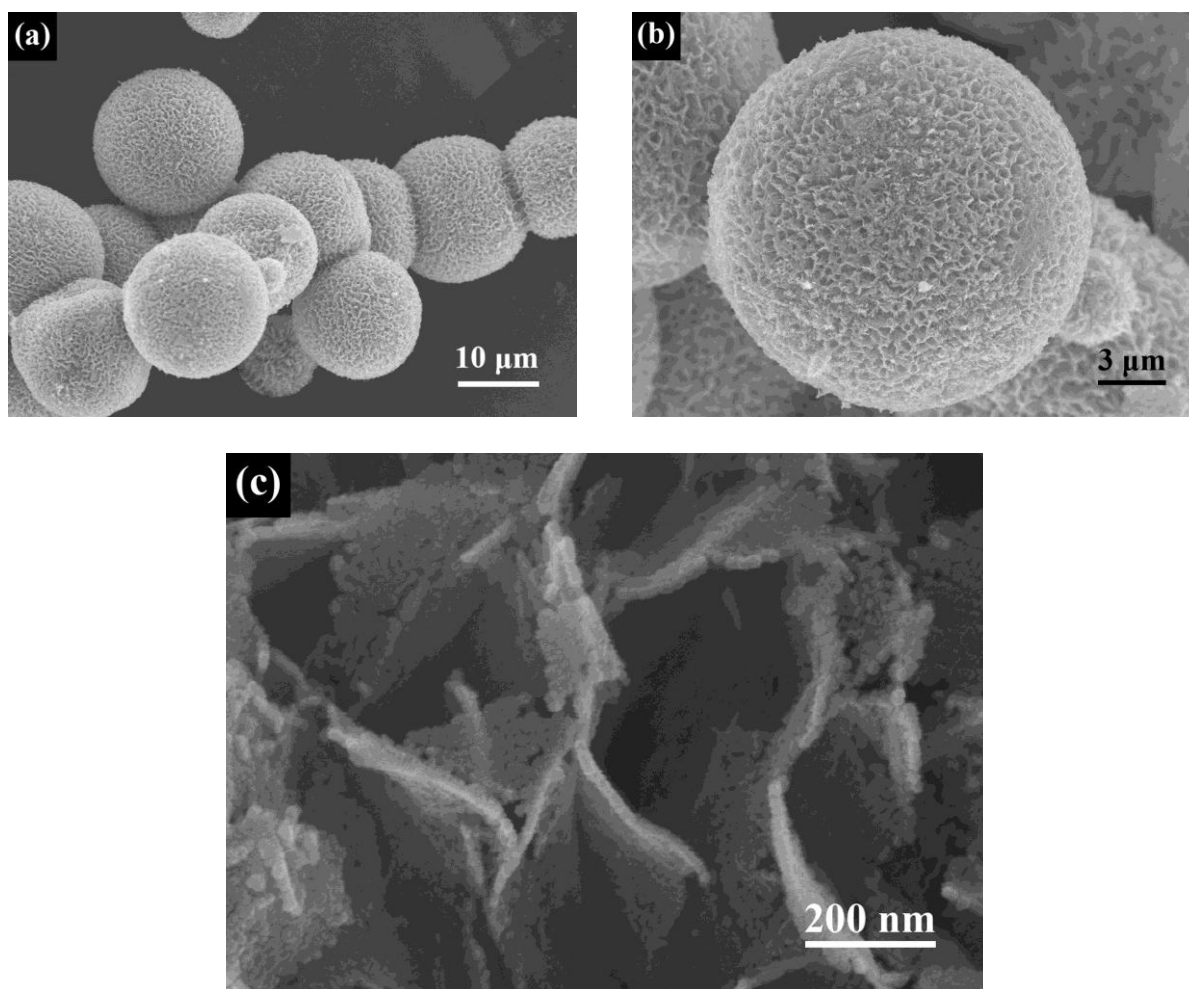


Figure 1. SEM images of the hierarchical structured ZnO microspheres, (a) the overall, (b) the single microsphere, and (c) the high magnification morphology.

Figure 1 presents typical SEM images of the ZnO products. The overall morphology in Figure 1a shows that ZnO primary particles have a perfect microspherical shape, and most of them are 15~20 μm in diameter. From the image of a single microsphere, as shown in Figure 1b, it can be seen that the microsphere has a porous structure, in which the pores are uniformly distributed. According to the high magnification image in Figure 1c, it is known that the microsphere is hierarchical, which is constructed by many secondary interconnected ZnO nanosheets. These nanosheets are micro-sized in length and widths, but only about 20 nm in thickness. Moreover, the ZnO nanosheet is mesoporous, and it is

composed of many tertiary nanostrips of about 20 nm in width. These nanostrips interconnect with each other, forming a two-dimensional network.

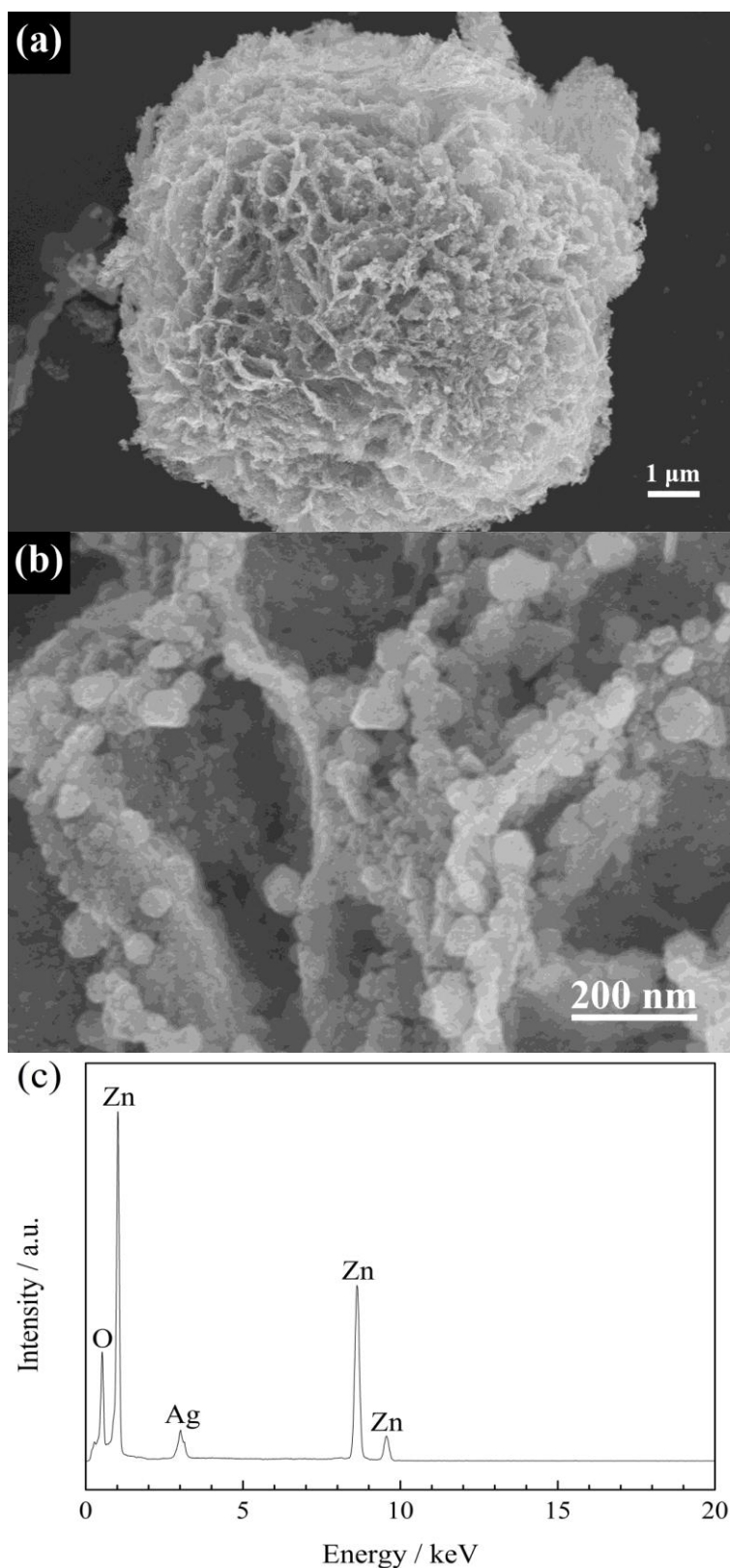


Figure 2. SEM images of the Ag decorated hierarchical structured ZnO microspheres, (a) the single microsphere, (b) the high magnification morphology, and (c) the corresponding EDS pattern.

Figure 2 is the SEM images after electroless silver plating. The spherical morphology preserves after the plating process (Figure 2a), but it can be seen that many nanoparticles, about 50 nm in size, are decorated uniformly on the ZnO microspheres (Figure 2b). The corresponding EDS pattern (Figure 2c) exhibits Zn, O and Ag peaks, and the mass content of Ag is about 6%.

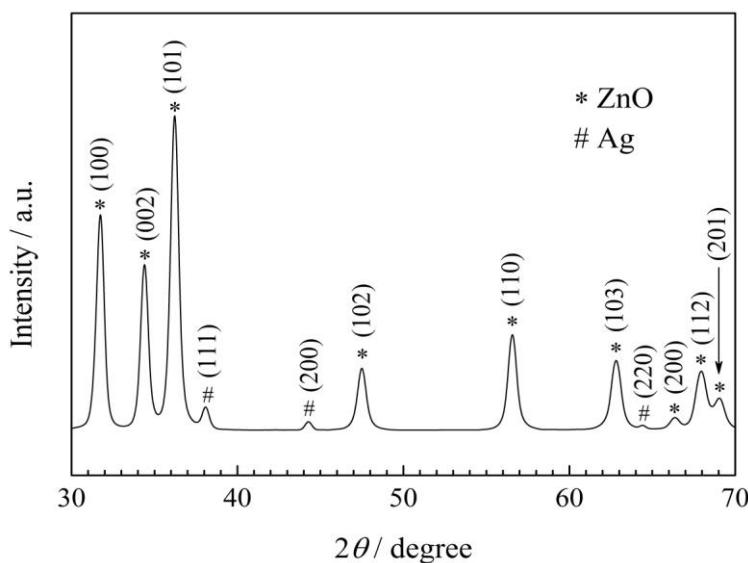


Figure 3. XRD pattern of the Ag decorated hierarchical structured ZnO microspheres.

Figure 3 is the XRD pattern after electroless silver plating. The diffraction peaks can be divided into two groups. One group at 31.7°, 34.4°, 36.2°, 47.5°, 56.6°, 62.8°, 66.3°, 68.0° and 69.0°, corresponds to the (100), (002), (101), (102), (110), (103), (200), (112) and (201) planes of wurtzite-type hexagonal ZnO, according to JCPDS No. 36–1451. The other group at 38.1°, 44.3° and 64.4°, corresponds to the (111), (200) and (220) planes of face-centered-cubic Ag, according to JCPDS No. 04–0783. Therefore, it can be concluded from these results that Ag decorated hierarchical structured ZnO microspheres are successfully prepared.

The electrochemical reactions between ZnO and Li are more complicated than other transition-metal oxides, according to the previous studies [8]. The reactions in the first discharge process can be written as follows.



Subsequently, the following charge and discharge reactions are reversible, including two reactions as below.



The electrochemical performance of Ag decorated hierarchical structured ZnO microspheres were studied as anode materials for lithium ion batteries. Figure 4 is the discharge-charge cycles at the current density of 100 mA g⁻¹ between 0.1 and 3 V. The discharge cut-off of 0.1 V is chosen because

the Li-alloying potential of Ag is below 0.1 V [23]. It can be seen that the first cycle is partially reversible, which is the common character of transition-metal oxides. The first discharge capacity is about 1180 mAh g^{-1} , higher than the theoretical value of 987 mAh g^{-1} calculated from equation (1) and (2). The extra capacity is caused by the solid electrolyte interface (SEI) layer, which is an organic layer consisting of ethylene-oxide-based oligomers, LiF, Li_2CO_3 , and lithium alkyl carbonate [5]. It forms in the discharge process with the consumption of some lithium, and it decomposes partially during the charge process [1–4].

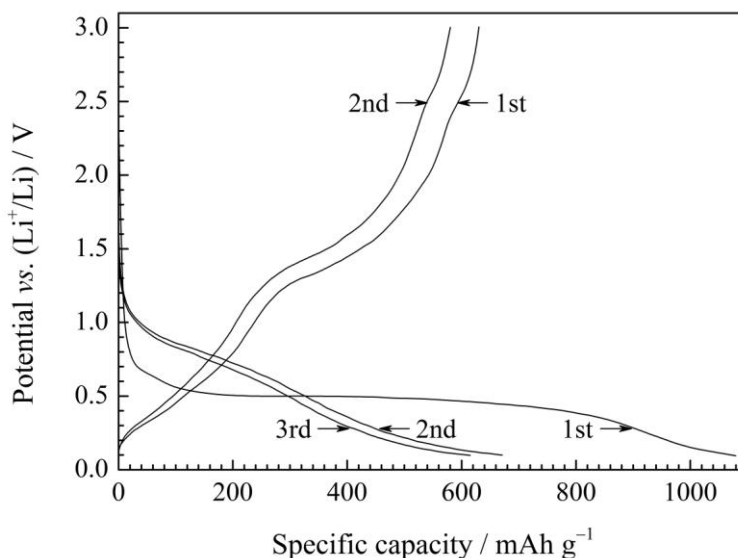


Figure 4. Discharge-charge curves of Ag decorated hierarchical structured ZnO microspheres at the current density of 100 mA g^{-1} .

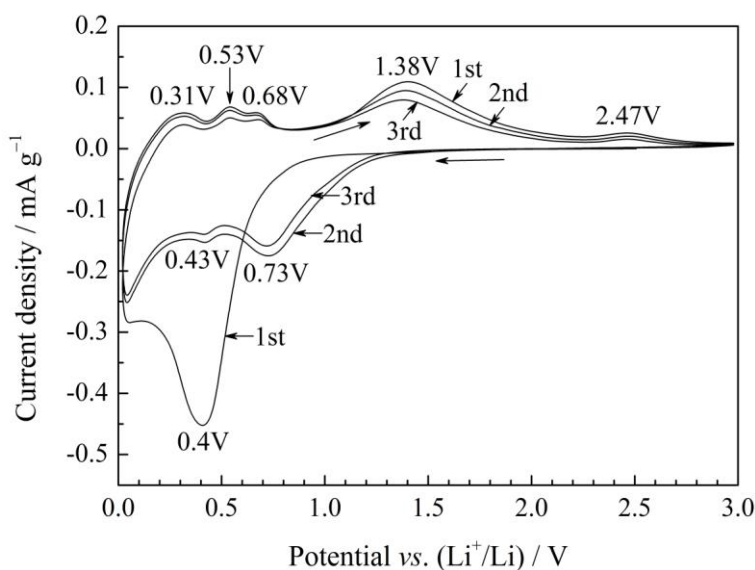


Figure 5. CV curves of Ag decorated hierarchical structured ZnO microspheres at the scan rate of 0.1 mV s^{-1} .

The first charge capacity is about 630 mAh g^{-1} , which is the reversible capacity. Obviously, the first discharge curve exhibits a long flat plateau appeared at about 0.5 V , but in the first charge curve, the plateau locates at a higher potential of about 1.4 V with much shorter length. The second discharge curve is quite different from the first one, where no obvious plateaus can be observed. The midpoint voltage is higher, indicating that the hysteresis becomes smaller and reversibility gets better.

Figure 5 is the cyclic voltammetry (CV) curves of Ag decorated hierarchical structured ZnO microspheres at a scan rate of 0.1 mV s^{-1} between 0 and 3 V . In the first cathodic scan, there is an obvious strong peak at 0.4 V . This peak is corresponding to the first electrochemical process of ZnO with lithium, including the reduction of ZnO to Zn, the alloying reaction between Li and Zn, and the formation of the SEI layer. In the first discharge, the potentials of these electrochemical reactions are very close, so it shows only a strong reduction peak. In the following anodic scan, five peaks can be seen. The first four peaks, located at $0.31, 0.53, 0.68,$ and 1.38 V , are related to the multi-step dealloying process of Li–Zn alloy. The other peak locates at 2.47 V , and it is related to the oxidation process of Zn back to ZnO [24, 25]. Since from the second scan, the curves become more reversible and show smaller hysteresis, which is in agreement with the discharge-charge curves. There are two peaks appeared in the following cathodic curves. The main peaks at 0.73 V are corresponding to the decomposition of ZnO and the formation of Li–Zn alloy, and the other at 0.43 V may be related to the formation of the SEI layer.

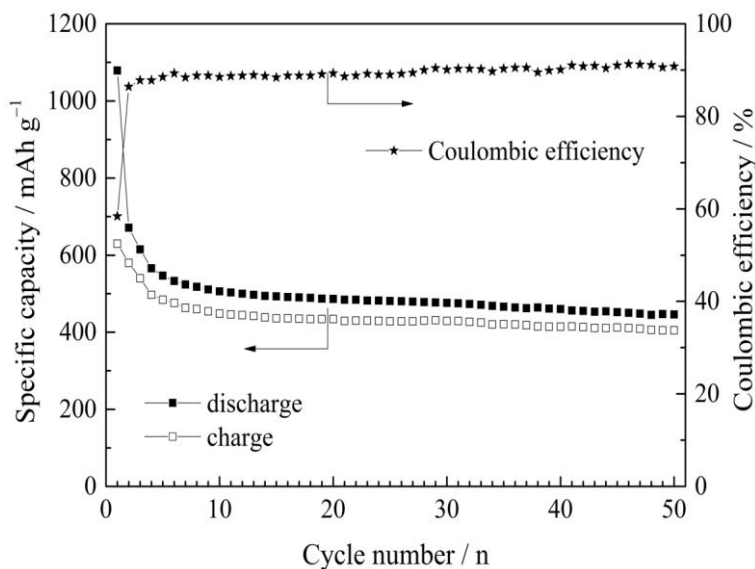


Figure 6. Cycling performance of Ag decorated hierarchical structured ZnO microspheres at the current density of 100 mA g^{-1} .

The discharge and charge capacities of Ag decorated hierarchical structured ZnO microspheres at 100 mA g^{-1} is presented in Figure 6. The capacities decrease rapidly in the first stage of cycle and then become more stable. The charge capacity after 50 cycles is 410 mAh g^{-1} , about 65% of the initial value. This value is much higher than many traditional electrodes made from ZnO powders [7, 13 and

16]. This indicates that the Ag decorated hierarchical structured ZnO microspheres have enhanced cycling performance.

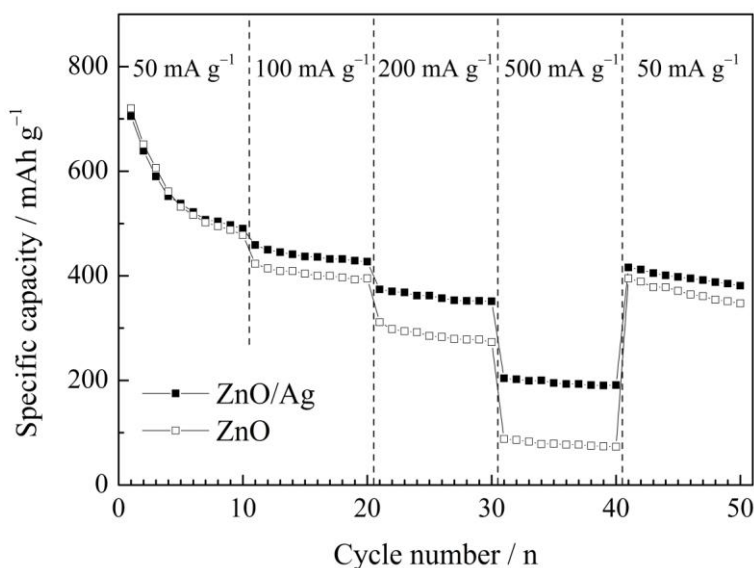


Figure 7. Comparison of rate capabilities of Ag decorated hierarchical structured ZnO microspheres and pure ZnO microspheres at different current densities.

The rate capability of Ag decorated hierarchical structured ZnO microspheres was investigated. The electrode was cycled at different current densities of 50, 100, 200, 500 and 50 mA g⁻¹ in turn, and at each stage it was cycled for 10 times. To make a comparison, pure hierarchical ZnO microspheres without Ag decorating are cycled together under the same conditions. Their charge capacities during the cycle are presented together in Figure 7. At the initial stage of 50 mA g⁻¹, the capacity differences between two electrodes are small. Both of the capacities drop quickly in this stage, but in the following stages, they become more stable. At 100 mA g⁻¹, the Ag decorated ZnO electrode exhibit higher capacities and its average capacity is 439 mAh g⁻¹, while for pure ZnO electrode, the average value is 404 mAh g⁻¹. It is obvious the capacity differences become larger at the higher current densities. At 200 mA g⁻¹, the average capacities for them are 360 and 287 mAh g⁻¹, respectively. At 500 mA g⁻¹, the capacities are 196 and 79 mAh g⁻¹, respectively. Finally, the current density returns back to 50 mA g⁻¹, their difference becomes smaller again, with the average values of 397 and 369 mAh g⁻¹, respectively. Therefore, it can be concluded that the rate capability of the hierarchical structured ZnO microspheres is enhanced by the decoration of Ag nanoparticles.

The enhanced electrochemical performance of Ag decorated hierarchical structured ZnO microspheres can be ascribed to the hierarchical structure of ZnO and the decoration of Ag nanoparticles. The hierarchical microsphere is porous, and it is constructed by many interconnected nanosheets. The nanosheet is mesoporous, which is composed of many interconnected nanostrips. This hierarchical porous structure contains numerous voids, which facilitate the access of electrolyte and ensure each particle can react fully with lithium. The hierarchical porous structure offers a much larger

specific surface area than the common irregular solid particles, and the open spacing between the nanosheets not only provides more sites for the adsorption of ions, but also promotes the fast electrochemical process of the active materials. The tertiary particles are only about 20 nm in size, so the diffusion path of lithium ions within the nanoparticle is as short as 10 nm. The hierarchical porous structure also has the ability of reducing the agglomeration and buffering the volume changes during the cycle. Moreover, after the silver plating process, ZnO microsphere was decorated by Ag nanoparticles. These Ag nanoparticles can greatly enhance the electrical contact between the ZnO nanosheets and reduce the contact resistance. All of these aspects are very important for the high capacity and rate capability of lithium ion electrode materials.

4. CONCLUSIONS

Ag decorated hierarchical structured ZnO microspheres are prepared by a hydrothermal method followed by an electroless silver plating technique. ZnO microspheres are constructed by many ZnO nanosheets, and the nanosheet is mesoporous, which is constructed by many interconnect ZnO nanostrips of about 20 nm. Ag nanoparticles with the sizes of about 50 nm decorate on the surfaces of the ZnO nanosheets, and its mass content is about 6%. As anode materials of lithium ion batteries, the Ag decorated hierarchical porous ZnO microspheres exhibit improved reversible capacity and enhanced cycling performance than many other electrodes made from ZnO powders. They also exhibit enhanced rate capability than the hierarchical ZnO microspheres without Ag decorating. It is believed that the enhanced electrochemical performance is attributed to the hierarchical structure of ZnO microspheres and the decoration of Ag nanoparticles.

ACKNOWLEDGEMENTS

This work is supported by National Natural Science Foundation of China (Grant No. 51204116) and Zhejiang Provincial Natural Science Foundation of China (Grant No. LQ14E02004). We would like to acknowledge them for financial support.

References

1. P. Poizot, S. Laruelle, S. Dupont and J. M. Tarascon, *Nature*, 407 (2000) 496.
2. S. Grugeon, S. Laruelle, R. Herrera-Urbina, L. Dupont, P. Poizot and J. M. Tarascon, *J. Electrochem. Soc.*, 148 (2001) A285.
3. P. Poizot, S. Laruelle, S. Grugeon and J. M. Tarascon, *J. Electrochem. Soc.*, 149 (2002) A1212.
4. A. Débart, L. Dupont, P. Poizot, J. B. Leriche and J. M. Tarascon, *J. Electrochem. Soc.*, 148 (2001) A1266.
5. G. Gachot, S. Grugeon, M. Armand, S. Pilard, P. Guenot, J. M. Tarascon and S. Laruelle, *J. Power Sources*, 178 (2008) 409.
6. Q. Xie, X. Zhang, X. Wu, H. Wu, X. Liu, G. Yue, Y. Yang and D. L. Peng, *Electrochim. Acta*, 125 (2014) 659.
7. X. H. Huang, X. H. Xia, Y. F. Yuan and F. Zhou, *Electrochim. Acta*, 56 (2011) 4960.
8. X. H. Huang, J. B. Wu, Y. Lin and R. Q. Guo, *Int. J. Electrochem. Sci.*, 7 (2012) 6611.

9. Q. Q. Xiong, Y. Lu, X. L. Wang, C. D. Gu, Y. Q. Qiao and J. P. Tu, *J. Alloys Compd.*, 536 (2012) 219.
10. X. Shen, D. Mu, S. Chen, R. Huang and F. Wu, *J. Mater. Chem. A*, 2 (2014) 4309.
11. T. Li, S. Ni, X. Lv, X. Yang and S. Duan, *J. Alloys Compd.*, 553 (2013) 167.
12. Z. Fang, W. Xu, T. Huang, M. Li, W. Wang, Y. Liu, C. Mao, F. Meng, M. Wang, M. Cheng, A. Yu and X. Guo, *Mater. Res. Bull.*, 48 (2013) 4419.
13. Z. Wu, L. Qin and Q. Pan, *J. Alloys Compds.*, 509 (2011) 9207.
14. K. T. Park, F. Xia, S. W. Kim, S. B. Kim, T. Song, U. Paik and W. I. Park, *J. Phys. Chem. C*, 117 (2013) 1037.
15. Y. N. Zhou, W. J. Li and Z. W. Fu, *Electrochim. Acta*, 59 (2012) 435.
16. W. T. Song, J. Xie, S. Y. Liu, Y. X. Zheng, G. S. Cao, T. J. Zhu and X. B. Zhao, *Int. J. Electrochem. Sci.*, 7 (2012) 2164.
17. S. M. Abbas, S. T. Hussain, S. Ali, N. Ahmad, N. Ali and S. Abbas, *J. Mater. Sci.*, 48 (2013) 5429.
18. X. H. Huang, J. B. Wu, Y. Lin and R. Q. Guo, *Int. J. Electrochem. Sci.*, 8 (2013) 1691.
19. J. Y. Xiang, J. P. Tu, L. Zhang, Y. Zhou, X. L. Wang and S. J. Shi, *Electrochim. Acta*, 55 (2010) 1820.
20. Q. Q. Xiong, J. P. Tu, Y. Lu, J. Chen, Y. X. Yu, Y. Q. Qiao, X. L. Wang and C. D. Gu, *J. Phys. Chem. C*, 116 (2012) 6495.
21. Q. Li, Y. Chen, T. Yang, D. Lei, G. Zhang, L. Mei, L. Chen and Q. Li, *Electrochim. Acta*, 90 (2013) 80.
22. L. Hu, Y. Sun, F. Zhang and Q. Chen, *J. Alloys Compd.*, 576 (2013) 86.
23. J. Morales, L. Sánchez, F. Martín, J. R. Ramos-Barrado and M. Sánchez, *J. Electrochem. Soc.*, 151 (2004) A151.
24. F. Belliard and J. T. S. Irvine, *J. Power Sources*, 97–98 (2001) 219.
25. J. Liu, Y. Li, X. Huang, G. Li and Z. Li, *Adv. Funct. Mater.*, 18 (2008) 1448.

© 2014 The Authors. Published by ESG (www.electrochemsci.org). This article is an open access article distributed under the terms and conditions of the Creative Commons Attribution license (<http://creativecommons.org/licenses/by/4.0/>).